电 化 学
J. Electrochem. 2022, 28(7), 2213001 (1 of 16)

[Review] DOI: 10.13208/j.electrochem.2213001 Http://electrochem.xmu.edu.cn

Research Progress of Copper Electrodeposition Filling Mechanism in Silicon Vias

Yun-Na Sun[1,2*], Yong-Jin Wu[1,2], Dong-Dong Xie[1,2], Han Cai[1,2], Yan Wang[1], Gui-Fu Ding[1*]

(*1. National Key Laboratory of Science and Technology on Micro/Nano Fabrication, Shanghai Jiao Tong University, Shanghai 200240, China; 2. School of Electronic Information and Electrical Engineering, Shanghai Jiao Tong University, Shanghai 200240, China*)

Abstract: Aiming at the electroplating filling problem of deep via TSV (through silicon via) interconnection, the multi-compatible integrated manufacturing technology team at the Shanghai Jiao Tong University has completed the numerical solution of the equations and realized the numerical simulation of TSV filling mode by applying the finite element method with arbitrary Lagrange Euler algorithm. The filling mechanisms of blind vias, the butterfly filling form for the through vias and the simultaneous filling mode of vias with different aspect ratios are analyzed by simulation, contributing to the parameter optimization and sample manufacturing. The effects of electroplating current density and heat treatment temperature on the mechanical properties of electroplating filled TSV-Cu were investigated by *in-situ* compression test and uniaxial film tensile test. With the increase of heat treatment temperature, the fracture strength and yield strength decreased significantly, and the Young's modulus changed slowly in a corrugated shape. The influence of the current density was more complexed. Based on the above research results, the thermal deformation mechanism of interconnection structure caused by thermal mismatch stress was studied through the self-built *in-situ* testing system, which gives change in the real-time deformation of TSV-Cu with temperature. The results showed that the thermal deformation process can be divided into the elastic deformation stage, the quasi plastic strengthening stage and the plastic deformation stage.

Key words: through silicon via; numerical simulation; Cu electrodeposition mechanism; arbitrary lagrange-eulerian; 2.5-dimension interposer

1 Introduction

With the continuous development of semiconductor industry, the volume of components and chips is getting smaller and smaller, but the volume of packaged components and chips is still large due to the limitation of packaging. Therefore, the improvement of packaging technology and the development of novel reliable technology have attracted extensive attention in the industry. Specially, the advanced package technology is of great essential for the chip, since it is directly related to the overall performance and subsequent application of chip. On the one hand, the chip must be isolated from outside to prevent impurities in the air from corroding the chip circuit, resulting in the decline of electrical performance. On the other hand, the encapsulated chip is also easier to be installed and transported. The packaging commonly used in the industry is 2-dimension packaging (also known as planar packaging, in which components and chip structure units are stacked and interconnected in parallel on the substrate), while 3-dimension (3D) packaging (wire bonding, flip chip, through sili-

Cite as: Sun Y N, Wu Y J, Xie D D, Cai H, Wang Y, Ding G F. Research progress of Cu electrodeposition filling mechanism in silicon vias. *J. Electrochem.*, 2022, 28(7): 2213001.

Received: 2022-02-18, Revised: 2022-03-28. *Corresponding author, Yun-Na Sun: (86-21)34670552, E-mail: Cecilia_Sun@sjtu.cn; Gui-Fu Ding: Tel: (86-21)34206686, E-mail: gfding@sjtu.edu.cn

con via (TSV) and film conductor)[1] can greatly improve the packaging density through interconnection in the *Z* direction, meeting the needs of multi-function and miniaturization[2-4].

As one of the advanced 3D packaging technologies, 3D TSV packaging has broad development prospects[5-7]. TSV technology is a subversive technology, which has become an important research direction, and solution to continue and expand Moore law through the filling of conductive materials such as Cu, tungsten and polysilicon. At present, TSV technology is not mature, and is only applied to the production of a few high-end products. Developing an efficient and reliable through via electroplating filling process is of great urgency in TSV packaging technology. Specially, the investigation of Cu plating filling is more important owing to its wide utilization. The simulation of the Cu plating filling contributes to revealing the underlying mechanism[8-10], which is promising in adjusting and optimizing the TSV package design to improve the reliability and reduce the cost. Nonetheless, the development of the finite element analysis for via filling process is relatively slow.

TSV technology is still facing the challenges in thermomechanical and electrical reliabilities[11-13]. Of note, the properties of materials are affected by both the size effect and the manufacturing process at microscale (diameter 1 ~ 100 μm, depth 10 ~ 400 μm)[14, 15]. Mastering the electrical, thermal and mechanical properties of TSV-Cu at microscale is the basis to ensure its reliable connection. Therefore, it is particularly important to study the properties and thermomechanical reliability of TSV, and optimize the design of TSV accordingly.

2 Electrodeposition Mechanism

The electrodeposition of TSV concludes blind via filling form and through via filling form, which are described by Figure 1(a) and (b), respectively. Since the arbitrary Lagrange Euler algorithm (ALE) has the advantages of both interface accuracy (or fluid resolution) and the ability to track large deformation, it allows to move boundaries without using moving mesh to track the material.

In the ALE method, a referential configuration is designed to describe the interface motion, which can be mapped to the spatial configuration and the material configuration, as shown in Figure 1(c). And a referential coordinate is built up to identify mesh points, in this way, the via filling mechanism can be described by tracking the moving cathode surface with ALE method[16-18].

2.1 Blind via Filling Mode

2.1.1 △ Shape and 八 Shape Filling Mode

Void-free filling is a vital factor for evaluating the

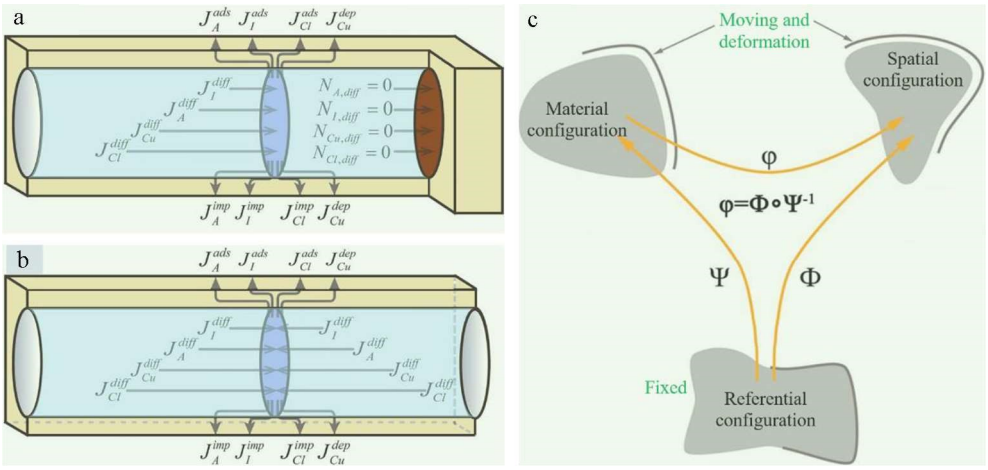

Figure 1 Transport-adsorption-desorption-incorporation models of (a) blind via, and (b) through via, (Reproduced with permission for Ref.[16], Copyright 2016, IOP Publishing, Ltd), (c) the mapping relations among the configurations of spatial, material, and referential.

quality of blind via filling. In order to achieve the void-free filling mechanism well, the typical comment defective filling models △ shape and 八 shape filling mechanism is analyzed in detail for the TSV with diameter of 40 μm and depth of 140 μm.

With the starting of the filling process, the concentration of Cu ion changes from the equal concentration distribution in the initial stage to decrease with via depth, and the decreasing range of the bottom concentration is the largest, as shown in Figure 2(a). The difference of Cu ion concentration leads to the decrease of current density (CD) at the bottom of the via, as illustrated in Figure 2(b). And the much higher CD will lead to a much higher deposition at the TSV orifice than that at the bottom of the via. Thus, the Cu deposited at the orifice will contact and seal together in advance, which will hinder the transports of accelerator and Cu ions to the via, weakening the deposition rate at the bottom of the via, and eventually forming a pore shown in Figure 2(c).

Considering the CD distribution of △ shape, the CD shall be adjusted to the situation that the CD at the bottom shall not be less than that at the orifice. The conventional method is to introduce inhibitor to regulate the deposition rate of Cu at the orifice, which obviously suppresses the deposition ability of the orifice demonstrated in Figure 3. The CD of the orifice is limited, since the surface coverage of accelerator is reduced with the increased coverage of inhibitor at the orifice given in Figure 3(b)-(d). Accordingly, the Cu ion concentration is also increased slightly. However, the deposition rate in the middle of the via is higher than that at the bottom, which leads to the early closure of the middle and leaves a hole at the bottom, as shown in Figure 4. Therefore, the two typical kinds of CD distribution situations mentioned above need to be avoided.

2.1.2 V Shape Filling Mode

Considering the CD distribution situation of △ shape and 八 shape, the CD shall be adjusted to that

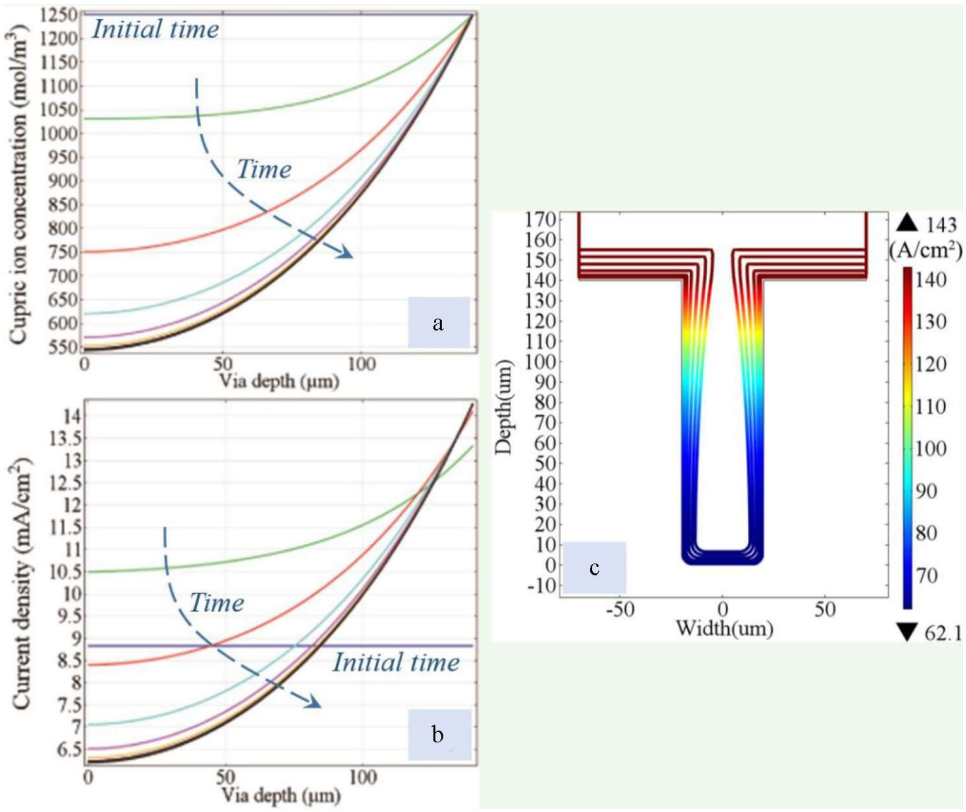

Figure 2 (a) Concentrations of cupric ion, and (b) CD, along the via depth direction; (c) filling profile and distribution of the CD, (Reproduced with permission for Ref.[17], Copyright 2015, IOP Publishing, Ltd.).

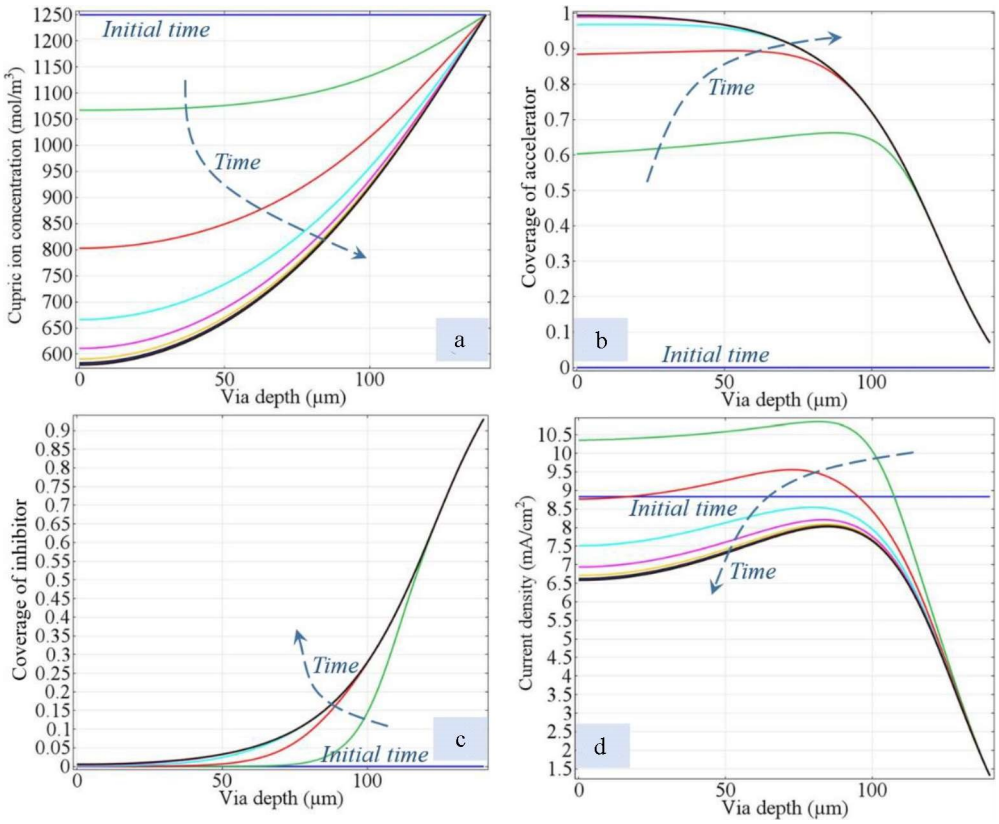

Figure 3 (a) Cupric ion concentration, (b) surface coverage of accelerator, (c) surface coverage of inhibitor, and (d) CD, along the via depth direction. Reproduced with permission for ref.[17], Copyright 2015, IOP Publishing, Ltd.

the CD is increased with the depth of the via. There fore, the inhibitor and accelerator are introduced to gether to regulate deposition rate of Cu at the orifice and bottom for the TSV with diameter of 40 μm and depth of 140 μm.

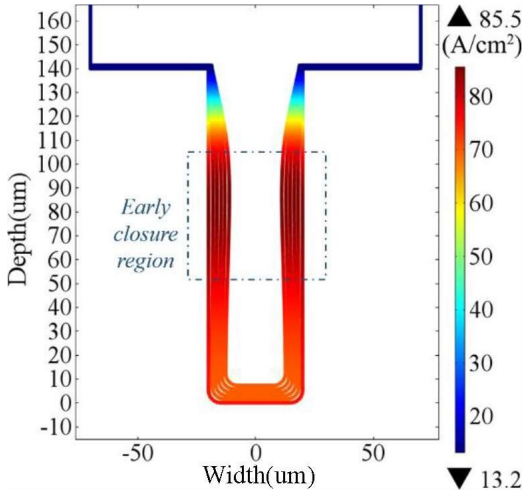

Figure 4 Filling profile and distribution of the CD. Reproduced with permission for Ref.[17], Copyright 2015, IOP Publishing, Ltd.

The inhibitor is mainly adsorbed in the orifice area, and the accelerator can quickly diffuse to the middle and bottom of the via by regulating the proportion of the inhibitor and the accelerator, because the diffusion coefficient of accelerator is much larger than that of inhibitor, and the adsorption rate constant of inhibitor is much larger than that of activities. Under this guidance, the proportion of inhibitor shall be increased to reduce the deposition ration of the early closure region of 8 model. The simulated results of the V shape filling model are given in Figure 5 and Figure 6. Void-free filling mechanism has been achieved under the synergy of inhibitor and accelerator. The cupric ion concentration of the bottom in creases greatly, as shown in Figure 5(a). The coverages of accelerator and inhibitor are increasing or decreasing approximate linearly along the via depth with the proceeding the filling process, as shown in Figure 5

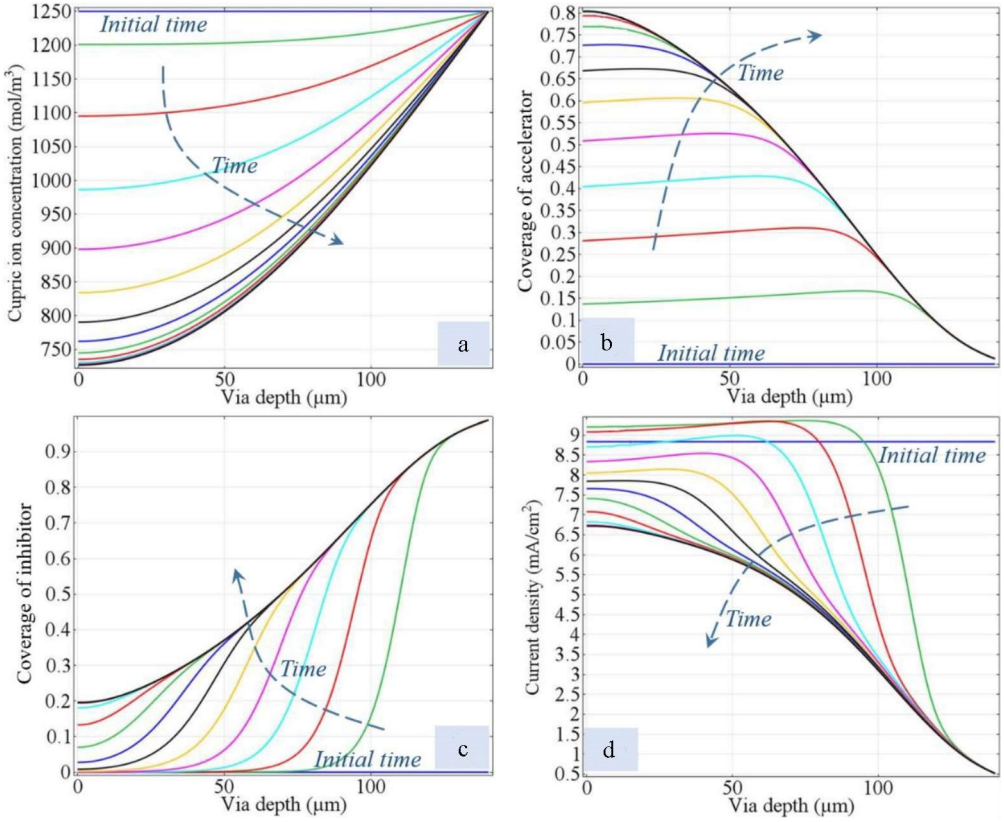

Figure 5 (a) Cupric ion concentration, (b) surface coverage of accelerator, (c) surface coverage of inhibitor, and (d) CD, along the via depth direction. Reproduced with permission for Ref. [17], Copyright 2015, IOP Publishing, Ltd.

(b) - (c). The suppressed area in the orifice is enlarged, and higher surface coverage inhibitor restrains the deposition rate in the orifice area of blind via, contributing to the formation of void-free filling mode.

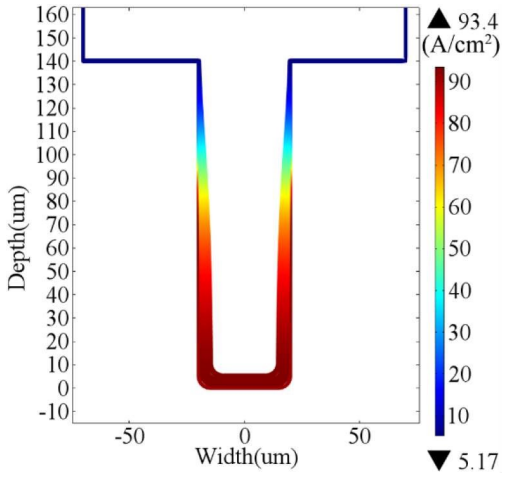

Figure 6 Filling profile and distribution of the CD. Reproduced with permission for Ref. [17], Copyright 2015, IOP Publishing, Ltd.

The CD increases gradually along the via depth, which is conducive to the formation of "V" filling mode given in Figure 5 and Figure 6.

2.1.3 Bottom-up Filling Mode

Bottom-up filling mechanism will be formed in an extremely higher proportion, since the deposition rates of orifice and side-wall can be completely limited. When the plating solution contains only 6 ppm inhibitor, the filling mode for TSV with diameter of 40 μm and depth of 140 μm shows a bottom-up filling mode given in Figure 7. The cupric ion concentration at the bottom is basically the same as that at the orifice. In the initial stage, there is a lack of inhibitor in the via due to the small diffusion coefficient and large adsorption rate constant of the inhibitor. After the upper reaches saturation, the inhibitor diffuses downward along the via, as shown in Figure 7 (b). Therefore, the inhibitor adsorption saturation boundary gradually moves to the bottom of the via, resulting in the gradual concentration of CD in the bottom

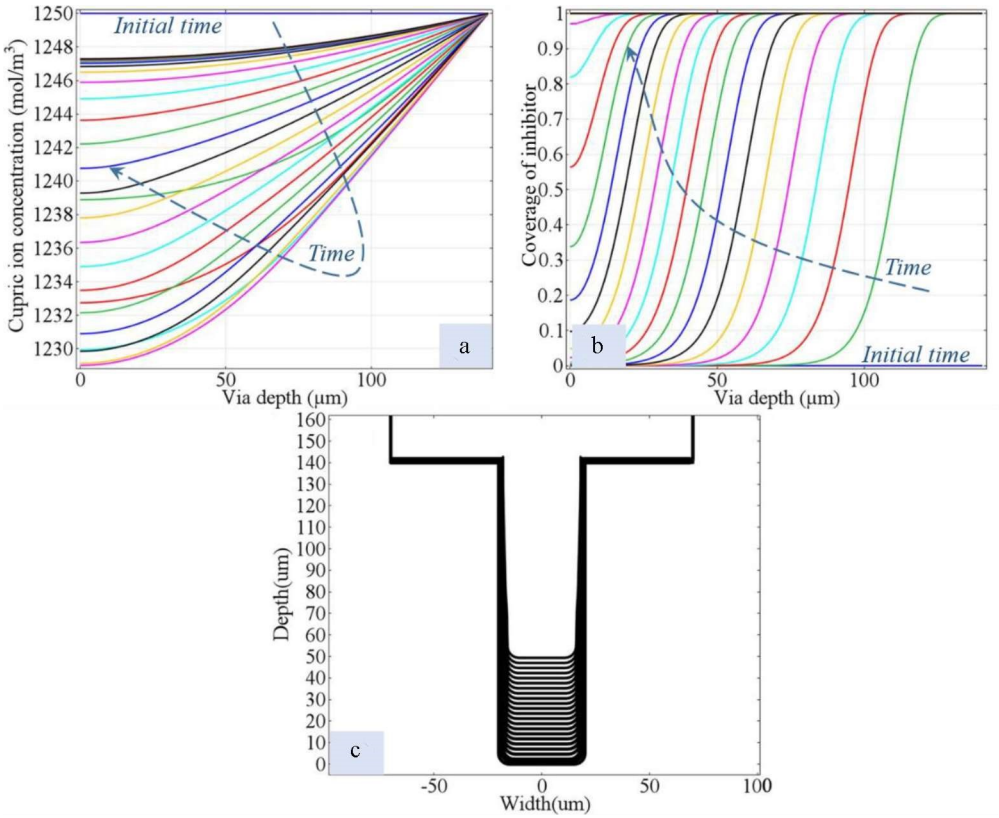

Figure 7 (a) Concentration of cupric ion, and (b) surface coverage of inhibitor, along the via depth direction; (c) Filling profile and distribution of the CD. Reproduced with permission for Ref.[17], Copyright 2015, IOP Publishing, Ltd.

area of the via. Finally, the inhibitors reach a steady state with the progress of diffusion. Furtherly, the in hibitor adsorbed at the bottom will desorb and form a bottom-up growth mode when the local CD is greater than the critical CD. Large deposition rate at the bottom is conducive to maintaining the bottom-up growth mode, which is promising for the extremely high aspect ratio vias and thin vias.

2.1.4 Copper Electrodeposition Samples for Different Modes

Figure 8 shows the experimental results of electroplating filling of corresponding blind vias, where the

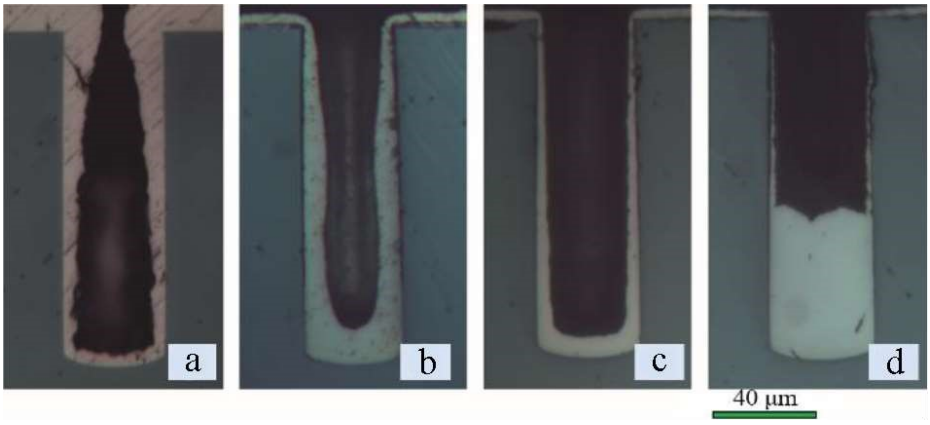

Figure 8 Cross-sectional images for (a) △, (b) ⋀, (c) V, and (d) bottom-up filling modes. Reproduced with permission for Ref.[17], Copyright 2015, IOP Publishing, Ltd.

filling forms of △ shape, 八 shape, V shape and bottom up shape are well matched with the simulation results, as exploited in Figure 2(c), Figure 4, Figure 6, and Figure 7(c), which proves the reasonability and reliability of the simulation of ALE methods. With this method, the filling process of TSV can be predicted, and the appropriate CD and additive ratio can be selected for different TSV sizes and structures.

2.1.5 Simultaneous Filling of Different Aspect Ratios Vias

In the 3D TSV package system, sometimes the vias have different aspect ratios, which is more complex than the filling form of uniform aspect ratio. For the via with small aspect ratios, a well filling mode cannot satisfy the via with high aspect ratio shown in Figure 9. For different aspect ratios, there exist extreme differences in the most suitable electroplating current, and proportion of accelerator and inhibitor, which can be explained as follows. Firstly, the primary current distribution is determined by TSV size, seed layer thickness and initial current distribution. Secondly, the current distribution is redistributed by electrochemical polarization and the accelerator. Furtherly, the filling form is affected by the mass transfer restriction.

At the same time, the proportions of the accelerator and the CD are the same. Therefore, multi-step direct CD is proposed and optimized for simultaneous filling of different aspect ratios. Table 1 and Figure 10 show a cross-sectional image of Cu electrodeposited in TSV using two multi-step methods. Both of the two methods provide a promising way for simultaneous filling. Specially, the second method M2 saves more time for the vias with the aspect ratio of 3 ~ 6.

2.2 Through Via Filling Mechanism

2.2.1 Butterfly Filling Mode

Except the conventional blind via filling modes, the through via filling mechanism is also important

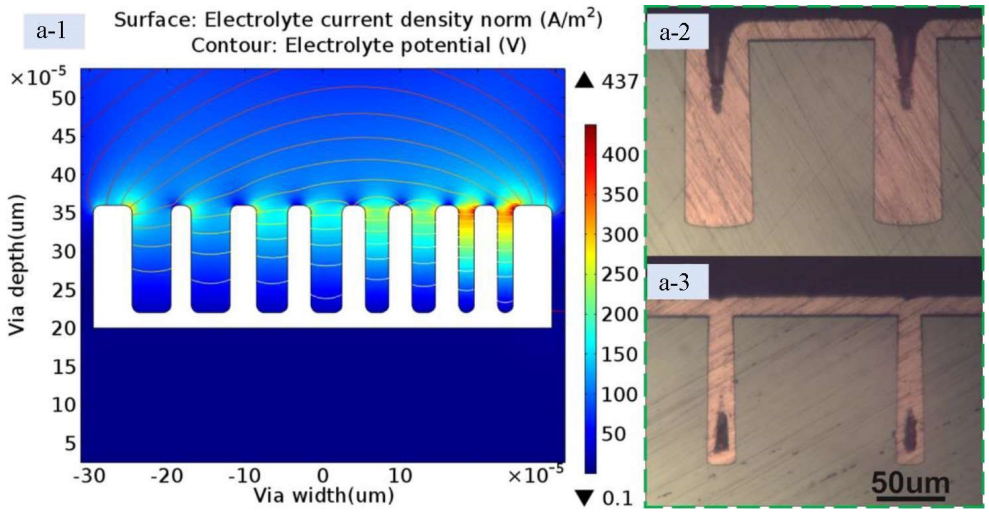

Figure 9 Simulation of electric field distribution in TSV (a-1) and TSV filling results (a-2, a-3)[19]

Table 1 Electrodeposition at different CDs and time Definition

Definition		Time range (min)	Current density (mA·cm^{-2})	Time range (min)	Current density (mA·cm^{-2})
M1	S1	0 ~ 60	1	60 ~ 120	3
	S2	120 ~ 150	6	-	-
	S3	150 ~ 180	6	-	-
M2		0 ~ 90	3	90 ~ 180	9

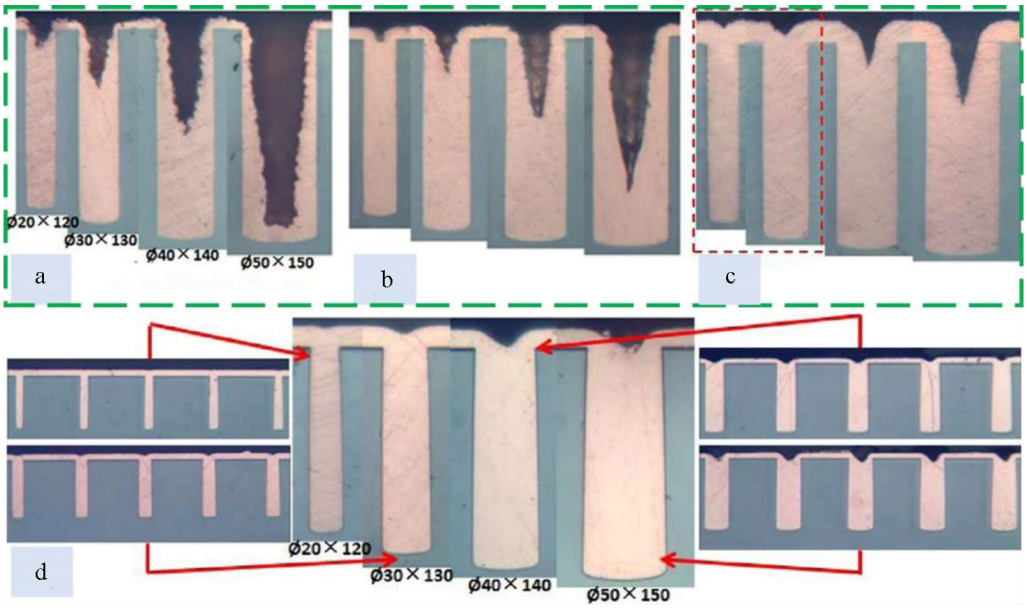

Figure 10 Cross-sectional images of TSV-Cu with different current densities (a) S1, (b) S2, and (c) S3. (d) M2. Reproduced with permission for Ref.[20], Copyright 2014, IOP Publishing, Ltd.

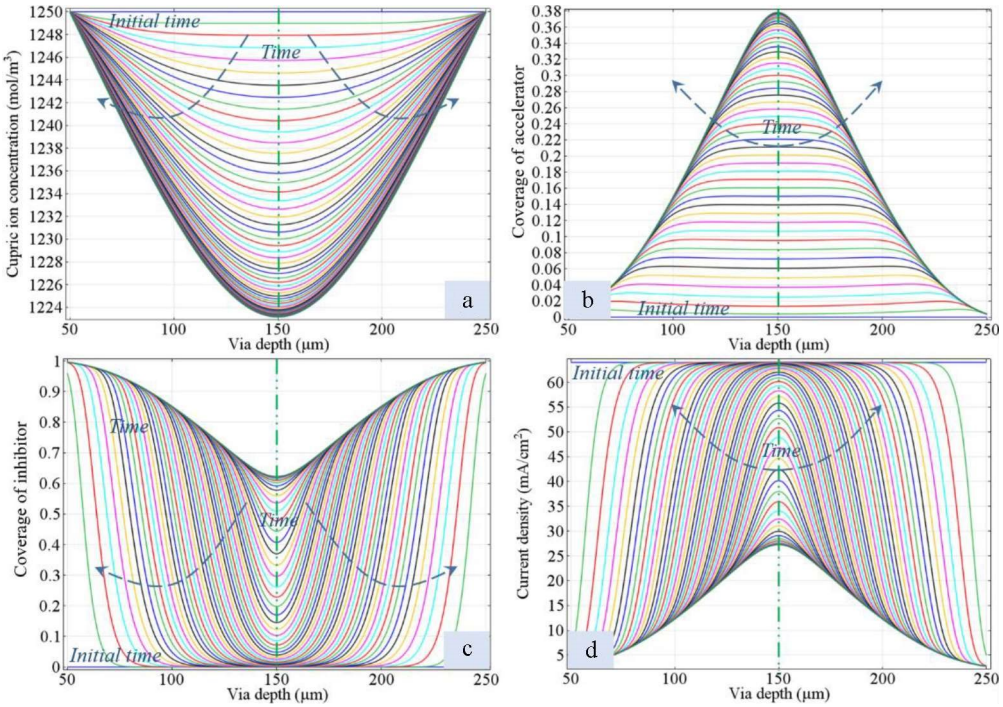

Figure 11 (a) Cupric ion concentration, (b) surface coverage of accelerator, (c) surface coverage of inhibitor, and (d) CD, along the via depth direction, (Reproduced with permission for Ref. [16], Copyright 2016, IOP Publishing, Ltd).

due to the time saving induced by bidirectional parallel filling. Therefore, the CD at the center of the through via needs to be much greater than that at the orifice. In addition, the deposition rate and consumption of Cu ions in the center are also the largest. Therefore, it is necessary to provide sufficient Cu ion diffusion to the center to compensate for consumption. The through via with diameter of 450 μm and

depth of 200 μm is analyzed in this section.

When the adjusted concentrations of accelerator and inhibitor are 0.2 ppm and 20 ppm, respectively, the cupric ion concentration reaches about 1224 mol·m^{-3}, which is close to the concentration at the orifice, as displayed in Figure 11(a). The accelerator diffuses and adsorbs in the center in advance, which accelerates the deposition rate of Cu in the center, as exhibited in Figure 11(b). This mechanism is formed by the delay in the diffusion of the inhibitor to the center, which provides sufficient diffusion time for the accelerator. The sufficient Cu ions of the center are realized by the inhibition formed by the inhibitor at the orifice, which indirectly provides sufficient Cu ions to be diffused to the center, as exposed in Figure 11(c). Due to the distribution forms of cupric ion, accelerator and inhibitor, the CD distribution is built up for void-free filling that the central area is much larger than the two orifices of 25 mA·cm^{-2} and 2 ~ 3 mA·cm^{-2}, as shown in Figure 11(d). Thus, the through via will form a butterfly filling mode with the progress of electroplating, as given in Figure 12. To sum up, the through vias with different aspect ratios can be filled in the form of butterfly by controlling the ratio of accelerator, inhibitor and CD in the plating solution. Through via electroplating is promising, since it has more competitive advantages than blind via electroplating. These advantages include saving electroplating time, reducing subsequent work steps and greatly improving the yield of TSV.

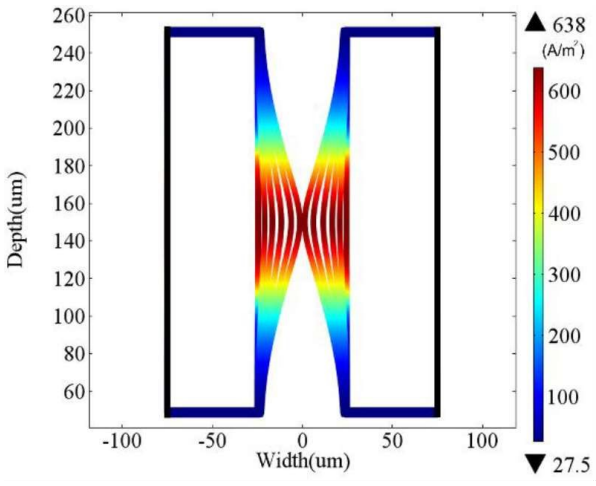

Figure 12 Filling profile and distribution of the CD, (Reproduced with permission for Ref.[16], Copyright 2016, IOP Publishing, Ltd).

2.2.2 Silicon Interposer

As a new fabrication process for silicon interposer, through silicon via filling mode together with dry film photoresist, is proposed to reduce the cost and improve the reliability[21, 22]. Both the time consumption and process cost are reduced greatly due to the simplified process.

As given in Figure 13(a), the TSVs with the pads are well fabricated by using the dry film photoresist. Uniform barrier layer and insulating dielectric layer are formed without chemical mechanical polishing process, as shown in Figure 13(b). It also shows stable resistance and electrical insulation, as well as a relatively low leakage current value of only ~ 1.43 × 10^{-13} A for TSVs with 220 μm pitch, which is much lower than the traditional value (10^{-12} ~ 10^{-9} A), as plotted in Figure 13(c).

2.2.3 Reinforced Polymer Interposer

Given to the challenges of silicon interposer including thermal-electrical-mechanical reliability, high cost and low yield, polymer interposer has attracted more attention owing to its simple technological process, low production cost and high production.

Copper reinforced polymer interposer and complex reinforced interposer are proposed, and fabricated with electroplating to improve their thermomechanical reliability, as given in Figure 14. When the Cu content of the composite is 40%, the Young's modulus and thermal conductivity are, respectively, about 4 times and 6 times higher than those of pure electrophoretic polymers, with the thermal expansion coefficient being 50% reduced. Thus, the thermal mismatch is weakened greatly. Further, given to the complex reinforced mechanism, the Young's modulus and thermal conductivity of the reinforced interposer are, respectively, about 1.2 times and 1.5 times those of the traditional, with about 90% of the coefficient of thermal extension remained. It is indicated that the incorporation of disordered SiC-whiskers, which reduces the mismatch between nickel (Ni) and

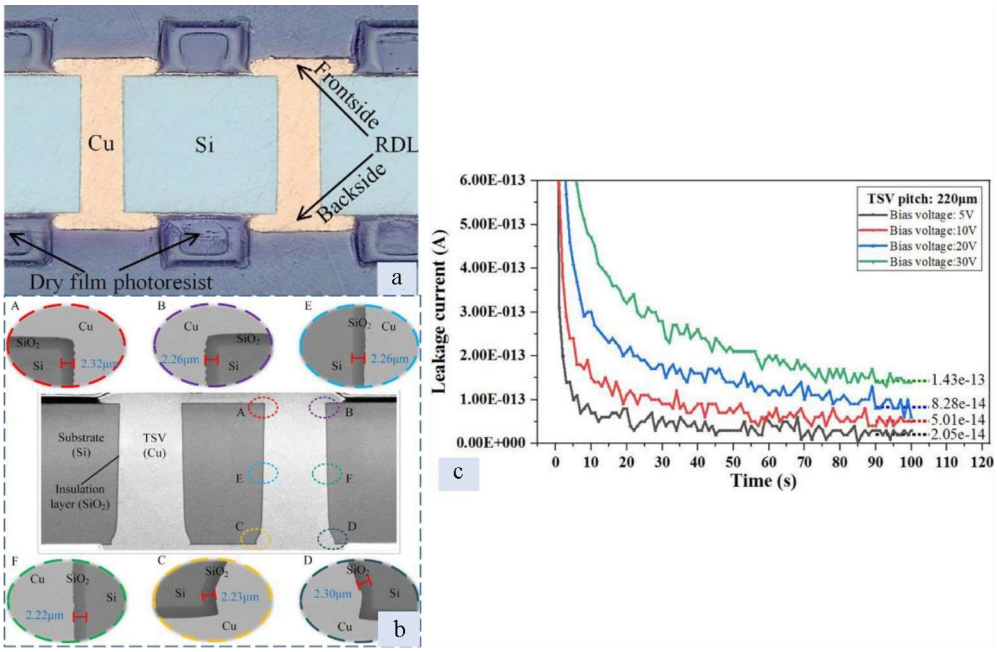

Figure 13 (a) and (b) Silicon interposer cross-sectional images, and (c) leakage current plots of TSVs, (Reproduced with permission for Ref.[22], Copyright 2018, IOP Publishing, Ltd).

polyimide (PI), improves the comprehensive properties of the polymer interposer according to the experimental results. Therefore, the co-use of ordered Ni grids and disordered SiC-whiskers/PI will be an innovative way to speed up the evolution of polymer interposer.

3 Mechanical Properties of TSV-Cu

Considering the small size of TSV (diameter 1 ~ 100 μm, depth 10 ~ 400 μm), the material properties of TSV-Cu are affected by both the size and the manufacturing process. Subsequently, the effects of CD applied in electroplating filling process and temperature load during heating process on the mechanical performance of TSV-Cu are mainly discussed.

3.1 Influence of Current Density

The influences of CD on the yield strength and microstructure of TSV-Cu were studied by *in-situ* compression test (Figure 15). The influence of CD of electroplating filling on the yield strength of TSV-Cu was tested by an independently built *in-situ* compression test device. TSV-Cu samples were prepared with different current densities (1 ~ 9 mA·cm^{-2}) under the same conditions as TSV electroplating filling. The Si substrate of the electroplated filled Cu was removed by etching process to obtain Cu samples (Figure 15 (b-1)). The samples were tested by *in-situ* compression test (Figure 15(b-2)) and the average value of the test data for the same standard samples was obtained, as shown in Figure 16. According to the test curve, the yield strength of TSV-Cu is 177.6 MPa @3 mA·cm^{-2}, which reaches the peak at the range 1 ~ 9 mA·cm^{-2}.

The microstructure is affected by the electroplated CD, which induces the change of yield strength. And the grain refinement occurred when the grain size decreased with the increased CD, as given Figure 16(b), so the yield strength increased with the CD increasing from 1 mA·cm^{-2} to 3 mA·cm^{-2}. As exhibited in Figure 16(c-d), the number of Σ3 grain boundaries also increased with the CD increasing from 1 mA·cm^{-2} up to 6 mA·cm^{-2}, and then decreased as it increased to 9 mA·cm^{-2} accompanying the increasement of Σ1 which has little contribution to the mechanical reinforcement. So, the yield strength would decrease with the CD increasing to 9 mA·cm^{-2}. Along with the increase of CD, the deposition amount of C element in the plating solution also increased, which may be the

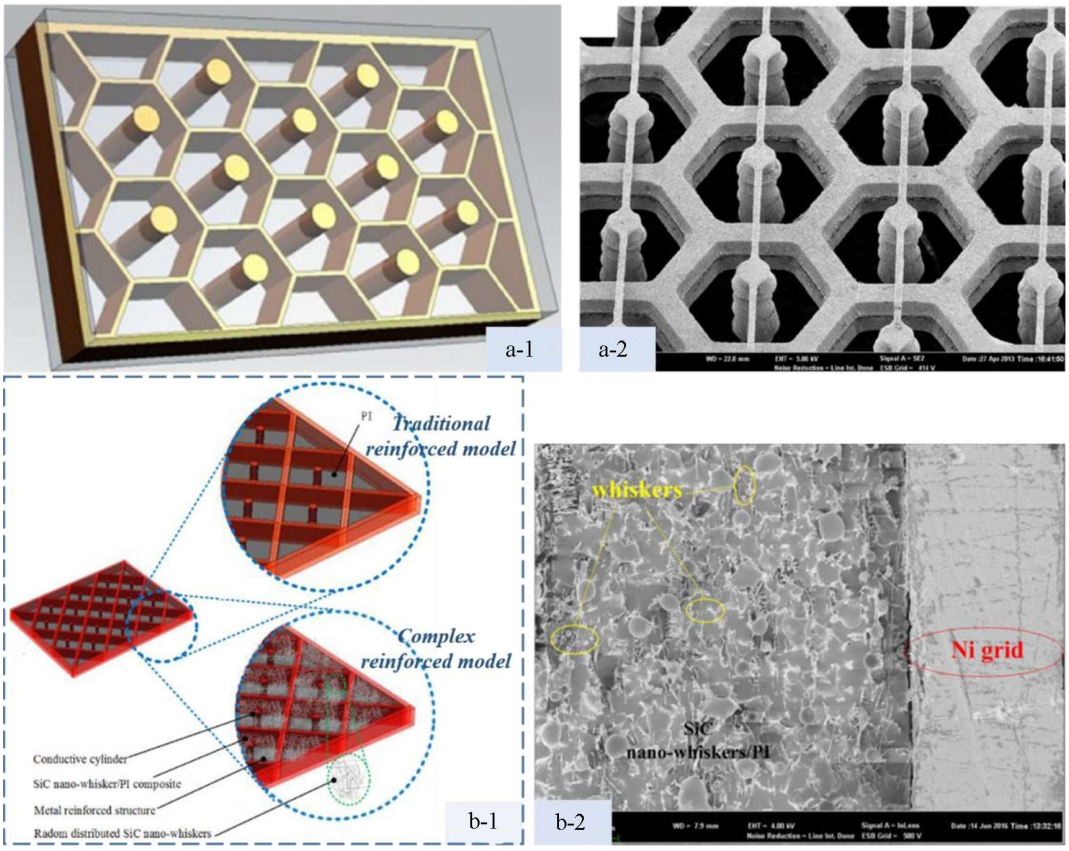

Figure 14 (a-1) Diagram, and (b-2) SEM image of Cu-ordered-reinforced interposer, (Reproduced with permission for ref.[23], Copyright 2014, IOP Publishing, Ltd), (b-1) diagram, and (b-2) SEM image of complex reinforced interposer, (Reproduced with permission for Ref.[24], Copyright 2017, Springer Nature).

factor leading to the decline in mechanical properties of materials.

3.2 Effect of Thermal Treatment

The Cu samples were prepared by using the same conditions as those of TSV electroplating filling (preparation of seed layer, electroplating CD, electroplating time, proportion of electroplating solution, etc.). To meet the requirements of tensile test, the electroplated film samples were etched. The prepared sample was placed in the dynamic mechanical thermal analyzer (DMA) system to be tested by uniaxial film tensile test, as shown in Figure 17(a). In this method, the influence of temperature load in heat treatment process on the TSV-Cu properties is analyzed. Figure 17(b) shows the changes of Young's modulus, yield strength and breaking strength of TSV-Cu samples at varied annealing temperatures.

It is visible that with the increase of heat treatment temperature, the fracture strength and yield strength of TSV-Cu decreased significantly, and the Young's modulus changed in a corrugated shape slowly. As shown in Figure 17(d) and Table 2, the (220) and (311) planes are the two main preferred orientations of the Cu samples. With the increase of the heat treatment temperature, the preferred orientations of (220) crystal plane became less evident, and eventually disappeared when the heat treatment temperature reached 200 ℃. Meanwhile, the preferred orientation of (311) crystal plane appeared after the heat treatment of 100 ℃, and those of (311) crystal plane became more and more obvious with the increase of the heat treatment temperature. The calculated value of Young's modulus changed with the increase of the heat treatment temperature, and the variation trend in the minimum value was almost consistent with that obtained in Figure 17(c). The difference

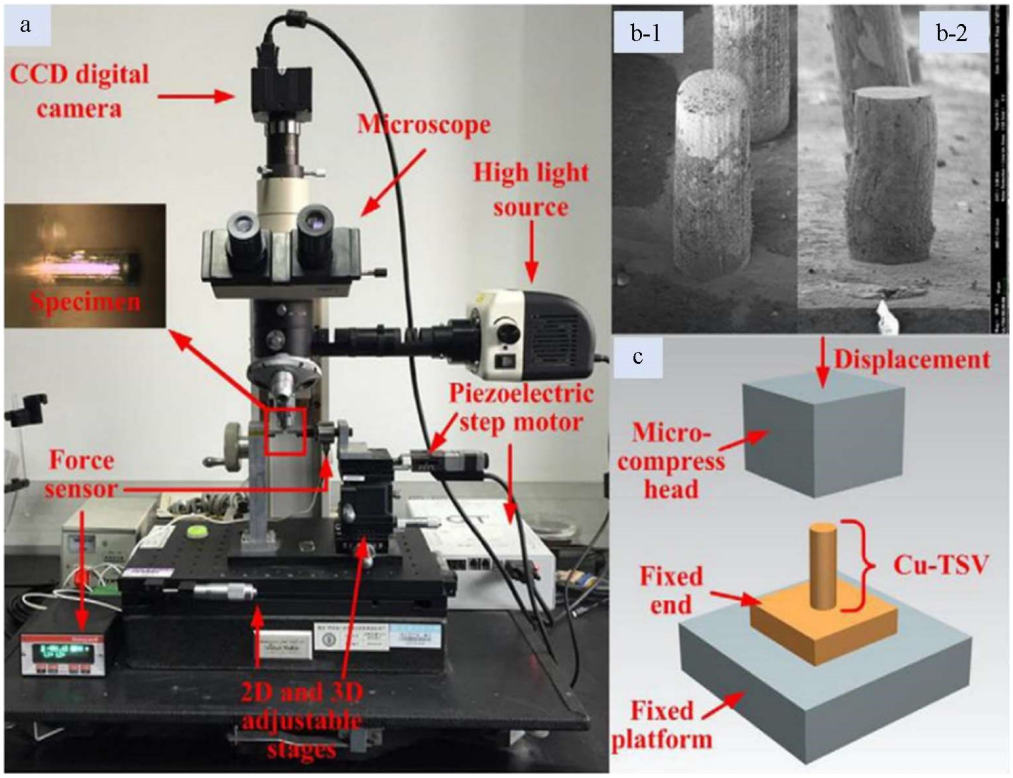

Figure 15 (a) Photograph of testing system; SEM images of Cu (b-1) before and (b-2) after the compression test; (c) diagram of the assembled samples used in the testing system, (Reproduced with permission for Ref.[15], Copyright 2015, Elsevier).

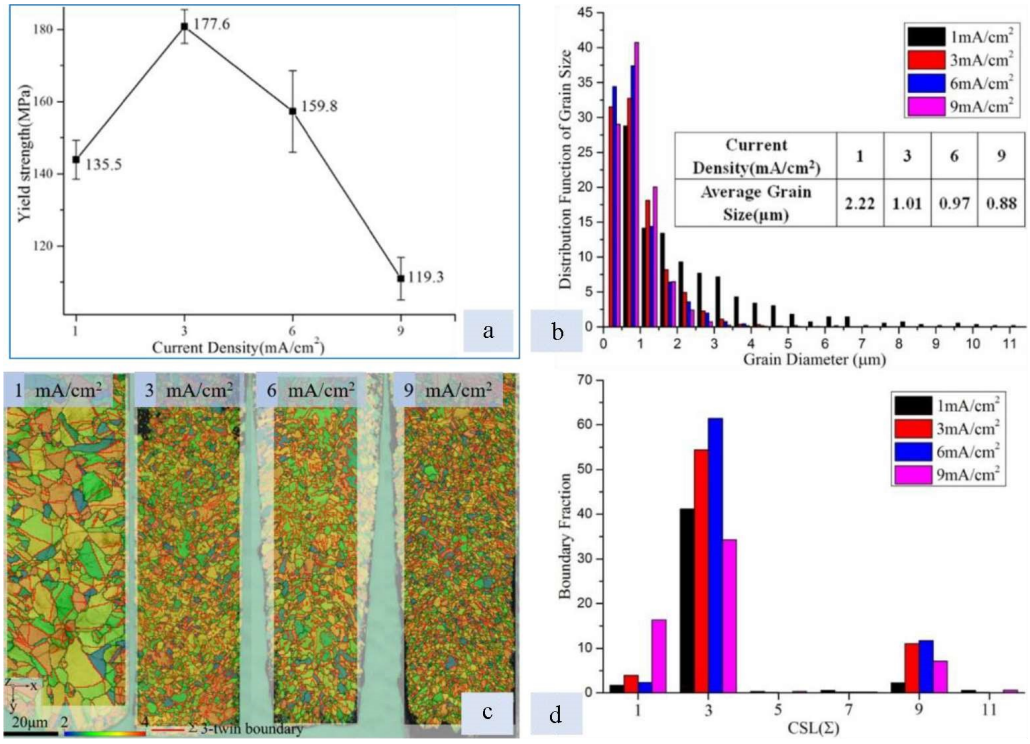

Figure 16 (a) Average yield strength, (b) grain size distribution, (c) Taylor factors and Σ3-twin boundary (the red lines), and (d) fraction of CSL boundaries of the Cu at different CDs, (Reproduced with permission for Ref.[15], Copyright 2015, Elsevier).

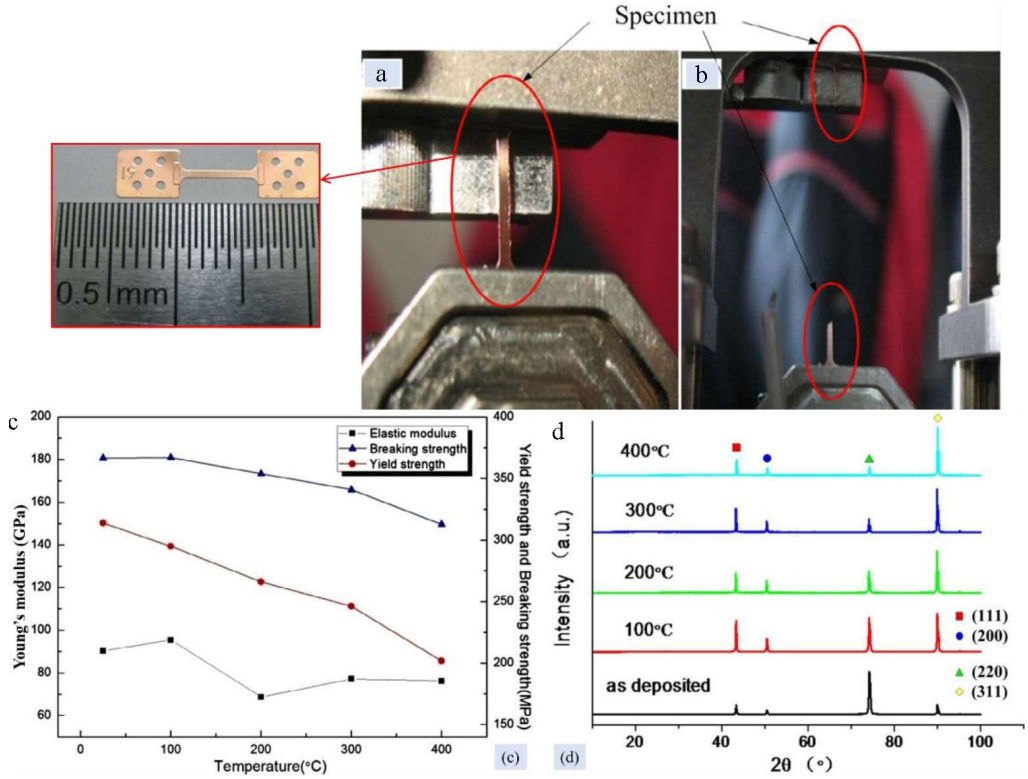

Figure 17 Photographs showing the specimen (a) before and (b) after the tensile test; (c) elastic modulus, yield strength and breaking strength plots, and (d) XRD patterns of the Cu specimens at different annealed temperatures. Reproduced with permission for Ref.[25], Copyright 2014, Elsevier.

Table 2 Texture coefficient and theoretical Young's modulus at different heat treatments[25]

		Room temperature	100 ℃	200 ℃	300 ℃	400 ℃
Crystal plane	(111)	0.028	0.058	0.042	0.055	0.040
	(200)	0.026	0.057	0.063	0.060	0.042
	(220)	0.753	0.389	0.278	0.190	0.123
	(311)	0.193	0.496	0.617	0.695	0.795
Young's modulus (GPa)		70.98 ~ 176.33	76.81 ~ 154.44	77.37 ~ 147.74	79.20 ~ 142.37	79.55 ~ 138.15

between the maximum and minimum Young's moduli also decreased, indicating that the increase of the heat treatment temperature makes the Young's modulus tend to be stable.

3.3 Transient Strain Characteristics Under Temperature Load

Based on the large difference in thermal expansion coefficient of TSV core structure, the thermal deformation mechanism of Cu was studied through the real-time observation by a self-built *in-situ* testing system given in Figure 18(a-b). The measured relative thermal deformation and effective deformation of the TSV specimens (Figure 18(c)) at different temperatures are given Figure 18(d). The thermal deformation can be divided into three stages, i.e., the elastic deformation stage (Stage I) occurring between 27 ~ 104 ℃, the quasi plastic strengthening stage (the critical stage, Stage II) occurring between

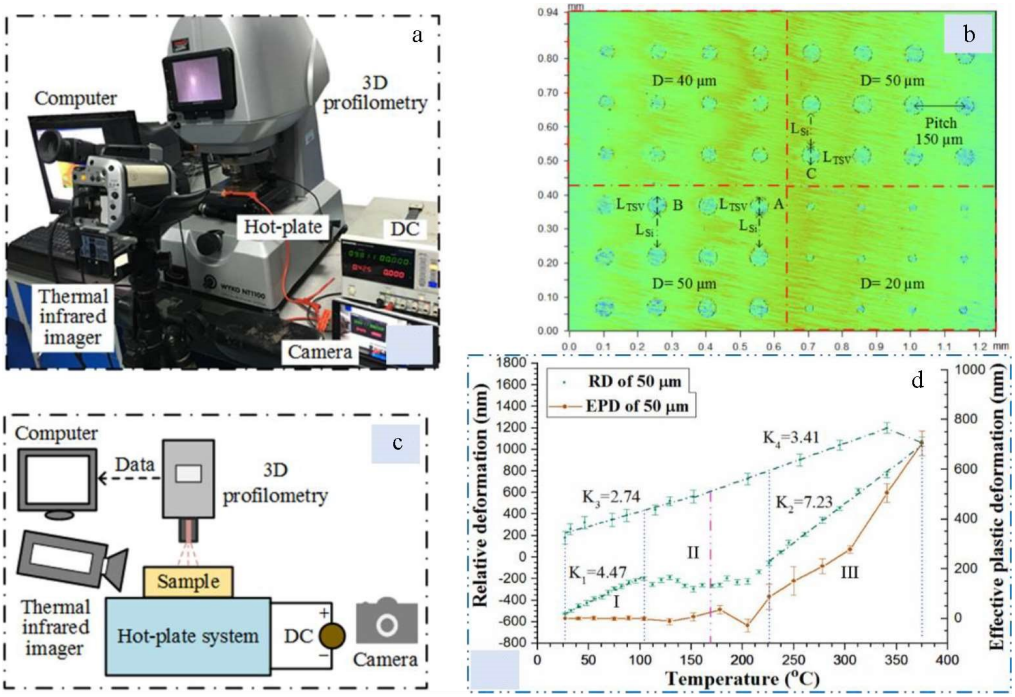

Figure 18 (a) and (b) *in-situ* testing system; (c) the samples, and (d) the average relative deformation (RD) and effective plastic deformation (EPD). Reproduced with permission for Ref.[26], Copyright 2017, IOP Publishing, Ltd.

104 ~ 226 ℃ and the plastic deformation stage (Stage III). In the indoor cooling stage, there are only two stages of elastic deformation and elastic-plastic deformation[26].

4 Conclusions

The numerical simulation of TSV deep through hole filling is realized by the combination of finite element method and ALE method, which agrees well with the experimental results. This proposed method was utilized to analyze the influence of via size and structure on the filling process and filling form of blind via. Accordingly, the electroplating filling process of through via in the butterfly form was successfully simulated.

The influences of electroplating CD and heat treatment temperature on the mechanical properties of TSV-Cu were analyzed. According to the *in-situ* compression test, the yield strength of TSV-Cu reached the peak (~ 177.6 MPa) at the CD of 3 mA·cm^{-2}. The uniaxial film tensile test results revealed that with the increase of the heat treatment temperature, the fracture strength and the yield strength decreased significantly, and the Young's modulus changed slowly in a corrugated shape.

Based on the comprehensive analysis in the influences of CD on TSV electroplating filling and TSV-Cu mechanical properties, the appropriate CD was selected to prepare TSV samples, and the thermal deformation caused by thermal mismatch stress was investigated. Through the self-built *in-situ* testing system, the variation of real-time deformation for the TSV-Cu with temperature was observed, which indicates that the thermal deformation can be divided into three stages: the elastic deformation stage, the quasi plastic strengthening stage and the plastic deformation stage.

Acknowledgements:

This work is supported by the National Key Research and Development Program of China (No. 2021YFB2011800) and Consultation and Evaluation Project of the Faculty of the Chinese Academy of Sciences (No. 2020-HX02-B-030).

References:

[1] Topper M, Baumgartner T, Klein M, Fritsch T, Reichl H.

Low cost wafer-level 3-D integration without TSV: 2009 Electronic Components & Technology Conference, San Diego, May 26-29, 2009[C]. Piscataway: IEEE, 2009.

[2] Katti G, Stucchi M, De Meyer K, Dehaene W. Electrical modeling and characterization of through silicon via for three-dimensional ICs[J]. IEEE Trans. Electron Devices, 2010, 57(1): 256-262.

[3] Kondo K, Suzuki Y, Saito T, Okamoto N, Takauchi M. High speed through silicon via filling by copper electrodeposition[J]. Electrochem. Solid-State Lett., 2010, 13(5): D26-D28.

[4] Wang F, Liu X M, Liu J Z. Effect of stirring on the defect-free filling of deep through-silicon vias[J]. IEEE Access, 2020, 8: 108555-108560.

[5] Pak J S, Ryu C, Kim J. Electrical characterization of trough silicon via (TSV) depending on structural and material parameters based on 3D full wave simulation: 2007 International Conference on Electronic Materials and Packaging, Daejeon, November 19-22 2007[C]. Piscataway: IEEE, 2007.

[6] Ho S, Yoon S W, Zhou Q, Pasad K, Lau J H. High RF performance TSV silicon carrier for high frequency application: 2008 Electronic Components & Technology Conference, Lake Buena Vista, May 27-30, 2008[C]. Piscataway: IEEE, 2008.

[7] Frank T, Moreau S, Chappaz C, Leduc P, Arnaud L, Thuaire A, Chery E, Lorut F, Anghel L, Poupon G. Reliability of TSV interconnects: Electromigration, thermal cycling and impact on above metal level dielectric[J]. Microelectron. Reliab., 2013, 53(1): 17-29.

[8] Zhu Y, Bian Y, Xin S, Ma S, Jin Y F. Effect of additives on copper electroplating profile for TSV filling: 2012 International Conference on Electronic Packaging Technology & High Density Packaging, Guilin, August 13-16, 2012[C]. Piscataway: IEEE, 2012.

[9] Josell D, Moffat T P. Extreme bottom-up filling of through silicon vias and damascene trenches with gold in a sulfite electrolyte[J]. J. Electrochem. Soc., 2013, 160(12): D3035-D3039.

[10] Jin S, Wang G, Yoo B. Through-silicon-via (TSV) filling by electrodeposition of Cu with pulse current at ultra-short duty cycle[J]. J. Electrochem. Soc., 2013, 160(12): D3300-D3305.

[11] Ryu S K, Lu K H, Zhang X F, Im J H, Ho P S, Huang R. Impact of near-surface thermal stresses on interfacial reliability of through-silicon vias for 3D interconnects[J]. IEEE Trans. Device Mater. Reliab., 2011, 11(1): 35-43.

[12] Kuo C, Tsai H. Thermal stress analysis and failure mechanisms for through silicon via array: 13th InterSociety Conference on Thermal and Thermomechanical Phenomena in Electronic Systems, San Diego, May 30-June 1, 2012[C]. Piscataway: IEEE, 2012.

[13] Sun Y N, Sun S, Zhang Y Z, Luo J B, Wang Y, Ding G F, Jin Y F. Initial thermal stress and strain effects on thermal mechanical stability of through silicon via[J]. Microelectron. Eng., 2016, 165: 11-19.

[14] Wang H Y, Cheng P, Wang S, Wang H, Gu T, Li J Y, Gu X, Ding G F. Effect of thermal treatment on the mechanical properties of Cu specimen fabricated using electrodeposition bath for through-silicon-via filling[J]. Microelectron. Eng., 2014, 114: 85-90.

[15] Wang H Y, Cheng P, Wang H, Liu R, Sun L M, Rao Q L, Wang Z Y, Gu T, Ding G F. Effect of current density on microstructure and mechanical property of Cu micro-cylinders electrodeposited in through silicon vias[J]. Mater. Charact., 2015, 109: 164-172.

[16] Zhang Y Z, Sun Y N, Wang Y, Cheng P, Ding G F. Further research on the silicon via filling mechanism using an arbitrary lagrange-eulerian (ALE) method[J]. J. Electrochem. Soc., 2016, 163(2): D24-D32.

[17] Zhang Y Z, Sun Y N, Ding G F, Wang Y, Wang H, Cheng P. Numerical simulation and mechanism analysis of through-silicon via (TSV) filling using an arbitrary lagrange-eulerian (ALE) method[J]. J. Electrochem. Soc., 2015, 162(10): D540-D549.

[18] Zhang Y Z, Ding G F, Cheng P, Wang H. Numerical simulation and experimental verification of additive distribution in through-silicon via during copper filling process [J]. J. Electrochem. Soc., 2015, 162(1): D62-D67.

[19] Zhang Y Z. Study on the filling mechanism and technology of through via[D]. Shanghai: Shanghai Jiao Tong University, 2016.

[20] Wang Z Y, Wang H, Cheng P, Ding G F, Zhao X L. Simultaneous filling of through silicon vias (TSVS) with different aspect ratios using multi-step direct current density [J]. J. Micromech. Microeng., 2014, 24(8): 085013.

[21] Zhang Y Z, Wang H Y, Sun Y N, Wu K F, Wang H, Cheng P, Ding G F. Copper electroplating technique for efficient manufacturing of low-cost silicon interposers[J]. Microelectron. Eng., 2016, 150: 39-42.

[22] Luo J B, Wang G L, Sun Y N, Zhao X L, Ding G F. Fabrication and characterization of a low-cost interposer with an intact insulation layer and ultra-low TSV leakage current[J]. J. Micromech. Microeng., 2018, 28(12): 125010.

[23] Wang M, Cheng P, Li J H, Wang Y, Wang H, Ding G F, Zhao X L. Fabrication and performances of a novel copper-ordered-reinforced polymer composite interposer[J]. J. Micromech. Microeng., 2014, 24(2): 025016.

[24] Liu Y M, Sun Y N, Wang Y, Ding G F, Sun B, Zhao X L. A complex reinforced polymer interposer with ordered Ni grid and SiC nano-whiskers polyimide composite based on micromachining technology[J]. Electron. Mater. Lett., 2017, 13(1): 29-36.

[25] Wang H Y, Cheng P, Wang S, Wang H, Gu T, Li J Y, Gu X, Ding G F. Effect of thermal treatment on the mechanical properties of Cu specimen fabricated using electrodeposition bath for through-silicon-via filling[J]. Microelectron. Eng., 2014, 114: 85-90.

[26] Sun Y N, Wang B, Wang H Y, Wu K F, Yang S Y, Wang Y, Ding G F. *In-situ* measurement on TSV-Cu deformation with hotplate system based on sheet resistance [J]. Mater. Res. Express, 2017, 4(12): 125003.

硅通孔内铜电沉积填充机理研究进展

孙云娜[1,2*], 吴永进[1,2], 谢东东[1,2], 蔡 涵[1,2], 王 艳[1], 丁桂甫[1*]

(1. 上海交通大学, 微米纳米加工技术国家级重点实验室, 上海 200240, 中国;
2. 上海交通大学电子信息与电气工程学院, 上海 200240, 中国)

摘要: 上海交通大学多元兼容集成制造技术团队针对 TSV 互连的深孔填充电镀难题, 借助有限元软件和任意拉格朗日-欧拉算法, 完成了方程组的数值解算, 实现了 TSV 填充模式的数值仿真。利用有限元和任意拉格朗日-欧拉算法分析了盲孔的填充机制, 通孔的蝴蝶形式的电镀填充过程, 以及不同深宽比孔的同时填充模式,并利用仿真数据进行了样品的研制及参数优化。分析了电镀的电流密度和热处理温度对电镀填充 TSV-Cu 的力学属性的影响。通过原位压缩试验研究了电流密度对 TSV-Cu 的力学性能和显微组织的影响。利用单轴薄膜拉伸试验分析了热处理工艺对 TSV-Cu 材料属性的影响。结果表明, 随着热处理温度的升高, TSV-Cu 的断裂强度和屈服强度明显下降, 杨氏模量呈波纹状变化但变化趋势缓慢。基于上述研究结果, 研究了热失配应力所导致的互连结构热变形机制, 通过自主搭建的原位测试系统, 实时观测 TSV-Cu 随温度变化而产生的变形大小, 以研究影响 TSV-Cu 互连热应力应变的规律。 结果表明, TSV-Cu 的热变形过程分为弹性变形阶段、类塑性强化阶段以及塑性变形阶段。

关键词: 硅通孔; 数值模拟; 铜电沉积机理; 任意拉格朗日-欧拉; 2.5D 转接板